

Supporting Information

A porous framework infiltrating Li-O₂ battery: a low-resistance and high-safety system

Yi-Peng Zhang,^{ab} Yi-Qiu Li,^a Zhong-Hui Cui,^a Jia-Cheng Wang,^a Osamu Yamamoto,^c Nobuyuki Imanishi,^c and Tao Zhang^{*ab}

^aState Key Lab of High Performance Ceramics and Superfine microstructure, Shanghai Institute of Ceramics, Chinese Academy of Sciences, 1295 Dingxi Road, Shanghai, 200050, P. R. China. E-mail: taozhang@mail.sic.ac.cn

^bCenter of Materials Science and Optoelectronics Engineering, University of Chinese Academy of Sciences, Beijing 100049, P. R. China

^cDepartment of Chemistry, Faculty of Engineering, Mie University, 1577 Kurimamachiya-cho, Tsu, Mie, 514-8507

*Corresponding Author: E-mail: taozhang@mail.sic.ac.cn

Table of Contents

1.0 Experimental Section	3
1.1 LLZTO powders and ceramic discs.....	3
1.2 Li-Sn alloy anode.....	3
1.3 Porous LLZTO layer.....	3
1.4 MWCNT air cathode.....	3
1.5 liquid electrolyte.....	4
1.6 Cell Assembling.....	4
2.0 Electrochemical analysis and material characterization	4
2.1 Electrochemical measurement.....	4
2.2 SEM observation and EDS analysis.....	5
2.3 XRD measurements.....	5
2.4 XPS measurements.....	5
2.5 FTIR tests.....	5
2.6 Raman tests.....	5
3.0 Figures	6
Fig. S1 Characterizations of LLZTO discs.....	6
Fig. S2 The XPS spectra for the acid etched LLZTO powders and disc.....	7
Fig. S3 The SEM images for the morphological evolution of LLZTO surface at different time.....	8
Fig. S4 FTIR spectra of LLZTO discs with various acid-etching time.....	9
Fig. S5 The SEM image of LLZTO porous layer with a large magnification.....	10
Fig. S6 The experiment to assess the capability of the porous layer to soak liquid.....	11
Fig. S7 Heating experiments of GF separator soaked in TEGDME electrolyte.....	12
Fig. S8 Cycling profile of framework infiltrating Li-O ₂ battery with MPT.....	13
Fig. S9 <i>In-situ</i> gas analysis of framework infiltrating Li-O ₂ battery without TEMPO.....	14

1.0 Experimental Section

1.1 LLZTO powders and ceramic discs

The $\text{Li}_{6.4}\text{La}_3\text{Zr}_{1.4}\text{Ta}_{0.6}\text{O}_{12}$ (LLZTO, $x=0.6$) powders were prepared via conventional solid state reaction, from stoichiometric Li_2CO_3 (Aladdin Reagent, 99.995%), $\text{La}(\text{OH})_3$ (Aladdin Reagent, 99.95%), ZrO_2 (Aladdin Reagent, 99.99%), Ta_2O_5 (Aladdin Reagent, 99.8%) and a 15 wt.% excess of Li_2CO_3 for compensating volatile Li components during synthesis. The powders were ball-milled in an alcohol medium for 12 hours, using zirconia balls, and then heated in air at 900°C for 12 hours. Then the LLZTO dense pellets were prepared by the hot-pressing sintering technique followed by mechanical processing. Finally, the LLZTO ceramic discs with a diameter of 12 mm and a thickness of 0.8 mm was obtained.

1.2 Li-Sn alloy anode

Li-Sn composite was prepared by adding a certain amount of Sn powder in molten Li with continuous stirring and heating on a hot plate. Then, the molten Li-Sn alloy was cast on the LLZTO discs.

1.3 Porous LLZTO layer

The porous LLZTO layer was created by acid etching. Firstly, the 10 v.% aqueous solution of HCl was prepared, and then dropping 50 μL of the solution onto the surface of the LLZTO disc. After 40 minutes of acid treatment, the LLZTO disc was transferred into ethanol and left for 10 minutes. Subsequently, the LLZTO disc was rinse with ethanol, and immediately transferred into the small transition box of the Ar-filled glove box for drying under vacuum. After that, the LLZTO discs was vacuum-sealed and packed in the Ar-filled glove box for subsequent experiments.

1.4 MWCNT air cathode

The cathode was prepared by mixing MWCNTs (XFNANO, 8-15nm) and poly (vinylidene fluoride) with a weight ratio of 9:1 in appropriate NMP homogeneously and carbon paper as the current collector.

The cathode was dried in vacuum oven at 120°C for 24 h and then transferred into glovebox before use. The CNT loading of each cathode was about 0.15–0.25 mg.

1.5 liquid electrolyte

The High-purity TEGDME (99.99% anhydrous, Sigma-Aldrich) was dried using molecular sieves (4 Å) in an Ar-filled glove box. LiClO₄(Aldrich) was dried at 120°C under vacuum over several days. 2,2,6,6-tetramethyl-1-piperidinyloxy (TEMPO, Aldrich) and N-Methylphenothiazine (MPT, Aldrich) were purchased from Sigma-Aldrich. 50 mM TEMPO-1 M LiClO₄ in TEGDME , 50 mM MPT-1 M LiClO₄ in TEGDME and 1M LiClO₄ in TEGDME was obtained before experiment respectively.

1.6 Cell Assembling

The symmetric cells were assembled in an argon-filled glovebox (M-Braun, Germany). The cells were in Swagelok-type with pressure of approximately 10 N cm⁻² on the ceramic plates via springs. Li metal and Sn powders were mixed in the Ar box in a certain weight ratio, and transferred to a stainless-steel piece with a circular groove. Then the treated ceramic discs are attached to the stainless-steel piece whose groove is filled with melt Li-Sn alloy, and after cooled down, the anode is sealed with vacuum grease.

For comparison, coin cells containing redox mediators without LLZTO discs were fabricated. CR2032-type coin cells with holes for O₂ access were used as the holder. The amount of the liquid electrolyte was 100 μL, immersed in a glass fiber separator.

A Swagelok-type Li–O₂ battery was prepared in an Ar-filled glove box: the acid etched LLZTO disc painted with Li-Sn alloy was used as separator, 30 μL of electrolyte was added to the porous structure facing cathode side before the CNT placed on the side. To protect the anode, the LLZTO disc was tightly glued inside the Swagelok-type cell using the vacuum grease. The galvanostatic charge–discharge tests were conducted with the LAND battery testing system at room temperature in an O₂ glove box.

2.0 Electrochemical analysis and material characterization

2.1 Electrochemical measurement

Electrochemical impedance spectroscopy (EIS) measurements were performed in the frequency range from 1 MHz to 0.1 Hz with an amplitude of 10 mV by an Autolab instrument. Galvanostatic cycling was conducted using the LAND battery testing system with different current densities at room temperature.

All the electrochemical tests of Li-O₂ batteries were carried out in the O₂-glove box with a pressure of 1 atm. The current density and the capacity are normalized by the weight of the MWCNT. Galvanostatic cycling was carried out using the LAND battery testing system.

2.2 SEM observation and EDS analysis

The field emission scanning electron microscope (FE-SEM, SU8220) was used for observation of porous LLZTO layer, the anode/SSE interface, the cathode after cycling and EDS mapping analysis.

2.3 XRD measurements

X-ray powder diffraction (BRUKER AXS GMBH) was used to analysis the discharge product with Cu K α radiation at the angle range of 10-80°. After discharged or charged in pure O₂, the cathodes were extracted from the batteries and then sealed tightly for powder X-ray diffraction (XRD) measurements.

2.4 XPS measurements

The discharge products were analyzed by the X-ray photoelectron spectroscopy (Thermo Fisher Scientific ESCALAB 250). The samples were prepared in the argon-filled glove box.

2.5 FTIR tests

Fourier transform infrared (FTIR) analysis were carried out by a Thermo Fisher Scientific instrument of FT/IR-Nicolet iS5 from 4000 to 500 cm⁻¹. The FTIR tests were carried out in the Ar-filled glove box.

2.6 Raman tests

Raman tests were carried out to observe the LLZTO after cycling. The LLZTO disc was extracted from the Swagelok-type battery, and washed with DME.

3.0 Figures

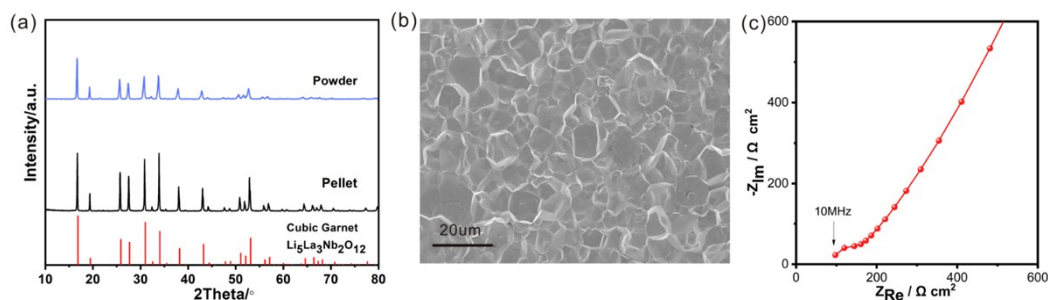


Fig. S1 | Characterizations of LLZTO discs. (a) XRD of LLZTO powder and dense electrolyte; (b) the SEM image of dense LLZTO; (c) EIS of the Au/LLZTO/Au symmetric blocking electrode system at room temperature. Au film coated on the LLZTO surface was prepared via magnetron sputtering. The overall resistance (Bulk and grain boundary) of LLZTO solid state electrolyte is about $115 \Omega \text{ cm}^2$. (b) The SEM image for the section of the LLZTO disc. The XRD patterns of prepared powders and ceramics, as shown in Fig. S1a, show a cubic garnet structure with no obvious impurity. In Fig. S1b, the LLZTO disc shows a dense cross-sectional structure, consistent with the Archimedes' test result, which indicates the relative density of the LLZTO disc is 99%. The impedance spectrum of the disc is given in Fig. S1c, and the ionic conductivity can be calculated from the spectrum, its value is $1.2 \times 10^{-3} \text{ S cm}^{-1}$.

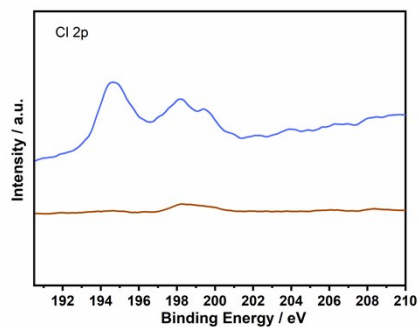


Fig. S2 | The XPS spectra for the acid etched LLZTO powders and disc. The top blue line represents the LLZTO powder after acid treatment (the HCl solution was dripped directly on the powder, and the powder was no longer rinsed with ethanol), the peaks related to chlorides can be observed, suggesting that the products of reaction of LLZTO with HCl are mainly chlorides. While, the bottom spectrum corresponding to the LLZTO disc shows an almost flat line without any obvious peaks, indicating that there is a small amount of chlorides remained.

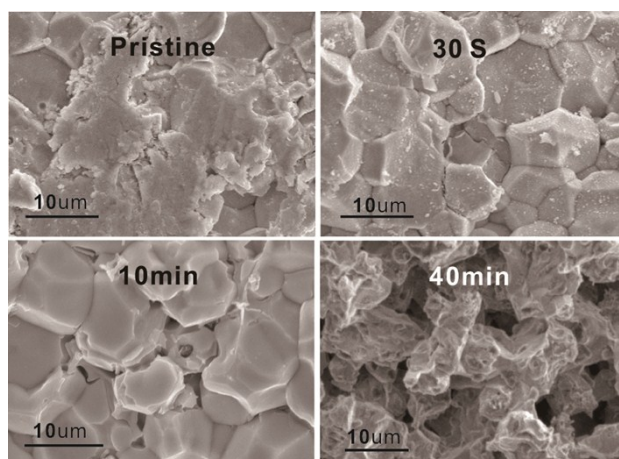


Fig. S3 | The SEM images for the morphological evolution of LLZTO surface at different time.

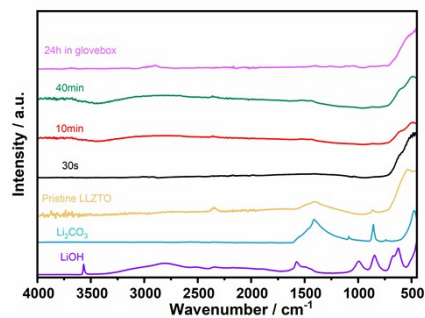


Fig. S4 | FTIR spectra of LLZTO discs with various acid-etching time. The two obvious peaks at 1440 and 863 cm⁻¹ confirm the presence of Li₂CO₃ on the surface of LLZTO disc polished by sandpapers. After a 30s-etching, these peaks disappear. When extending the etching time to 40 min, there is no obvious change in the FTIR spectra.

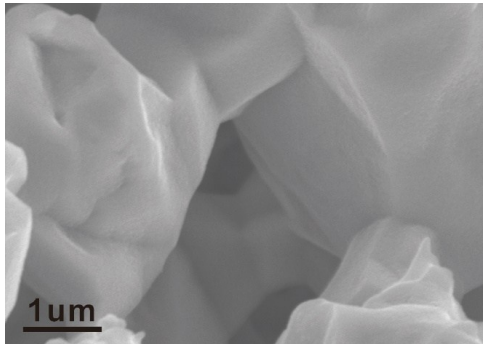


Fig. S5 | The SEM image of LLZTO porous layer with a large magnification. After acid etching for 40 min and washed with ethanol, the smooth surface of LLZTO grains can be observed, demonstrating that no significant amount of chloride produced by chloride remains on the surface.

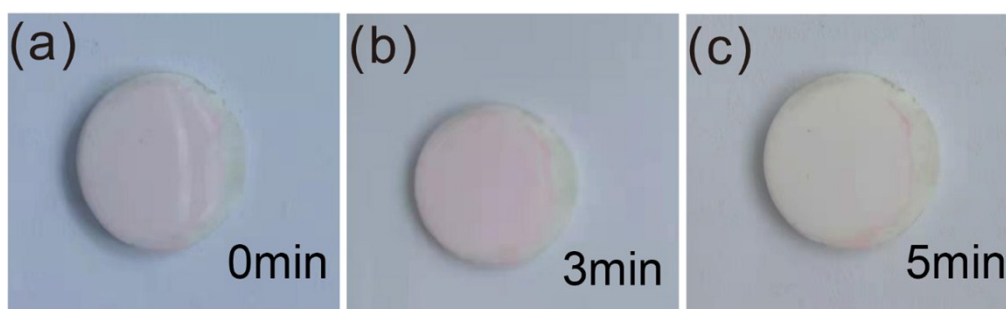


Fig. S6 | The experiment to assess the capability of the porous layer to soak liquid.

Photographs (a-b) show that a drop of red ink was dropped on the surface of the porous layer, and then the ink gradually seeped into the porous layer with the passage of time.



Fig. S7 | Heating experiments of GF separator soaked in TEGDME electrolyte.

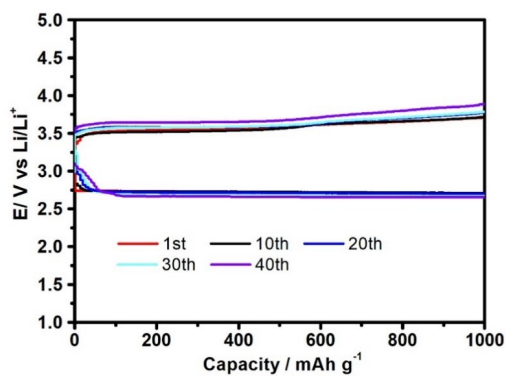


Fig. S8 | Cycling profile of framework infiltrating Li-O₂ battery with MPT. The battery is tested at a current density of 200 mA g⁻¹ with a limit capacity of 1000 mAh g⁻¹. The battery can cycle stably and keep charging voltage as low as 3.8 V after 40 cycles, which means that the battery constructed here is an appropriate platform where redox mediators can work well.

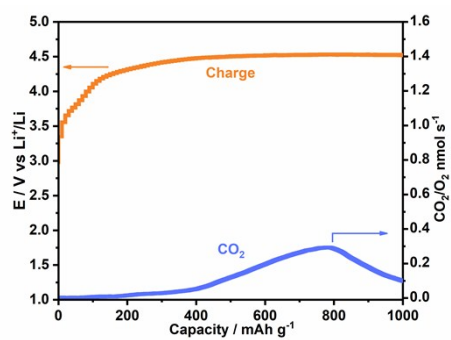


Fig. S9 | Charging curves and corresponding *in-situ* gas analysis of framework infiltrating Li-O₂ battery without TEMPO. The battery was tested under 200 mA g⁻¹ with fixed capacity of 1000 mAh g⁻¹, Ar flux is set as 1 mL min⁻¹.